Enhanced electrochemical properties of Co/CMK-3 composite as negative material for alkaline secondary battery

Li Li, Yanan Xu, Cuihua An, Yijing Wang*, Lifang Jiao, Huatang Yuan

Institute of New Energy Material Chemistry, Key Laboratory of Advanced Energy Materials Chemistry (MOE), Tianjin Key Lab of Metal and Molecule-based Material Chemistry, Nankai University, Tianjin 300071, PR China

H I G H L I G H T S

- Adding CMK-3 can remarkably enhance the electrochemical activity of the Co.
- The discharge capacity of the Co/CMK-3 (25 mg CMK-3) can reach 519.3 mAh g^{-1}.
- Co/CMK-3 (25 mg CMK-3) exhibits excellent cycle stability and rate capability.
- The capacity after 100 cycles was still 365.8 mAh g^{-1}.

A R T I C L E I N F O

A B S T R A C T

Co/CMK-3 composites are synthesized via a facile hydrothermal route. The electrochemical performances of Co/CMK-3 composite as the negative electrode material for alkaline rechargeable Ni/Co batteries have been systemically investigated. Electrochemical measurements show that the CMK-3 can remarkably enhance the electrochemical activity of Co, leading to a notable improvement of the discharge capacity, cycle stability and rate capability. Interestingly, the discharge capacity of Co/CMK-3 (25 mg CMK-3) electrode can reach 519.3 mAh g^{-1} and retains about 365.8 mAh g^{-1} after 100 cycles at discharge current of 100 mA g^{-1}. The electrochemical reaction mechanism of Co/CMK-3 composite electrode can be attributed to the electrochemical redox reaction between Co and Co(OH)$_2$.

1. Introduction

Alkaline rechargeable batteries are considered as one of the most promising energy storage applications due to their powerful and reversible electrochemical redox reactions. Recently, a new type alkaline rechargeable Ni/Co battery system using Ni(OH)$_2$ as cathode materials and Co-based materials as anode materials was systematically proposed [1]. The fabricated Ni/Co cell presents outstanding cycle stability, high rate capability and environmental friendly property. Thus, Ni/Co alkaline rechargeable batteries are widely explored and investigated in the following years.

As compared to cathode materials of Ni/Co batteries, recent researches mainly focus on anode materials. Up to now, extensive researchers have concentrated on Co-based materials as negative materials for Ni/Co batteries [2–8]. These Co-based materials, including Co–Si, Co–B, Co–P, Co–S, and Co–BN [9–14], have been

proved to be suitable for Ni/Co batteries. They demonstrated to have good electrochemical properties, including high discharge capacities, excellent cycle stabilities and rate capabilities. And the active material of these negative materials was proved to be metallic Co. In addition, Song et al. [15] reported that the nonmetallic material can improve the dispersion and increase the contact area between alkaline solution and active material. On the other hand, Co–carbon materials, such as Co–CNTs (hydrothermal) and Co–carbon nanotube (ball-milled) [16,17], have also been reported to show excellent electrochemical performances. As compared to the nonmetallic materials in above Co-based materials, carbon can not only improve the dispersion of materials, but also the electroconductibility of materials [18,19]. CMK-3, as an ordered mesoporous carbon [20,21], has notably improved the electrochemical performances of LiFePO$_4$ [22]. As compared to carbon nanotube, CMK-3 with high surface area may be a better matrix material. Furthermore, the BET surface areas and morphology of cobalt-based materials are the most important factors influencing the discharge capacity, which are largely dependent on the contact area between the electrode and

* Corresponding author.
  E-mail address: wangyj@nankai.edu.cn (Y. Wang).

alkaline aqueous [23–25], i.e. the content of CMK-3 will determine the rate performance, conductivity and discharge capacity of the battery [26]. Therefore, the content of CMK-3 and BET surface areas of Co-based materials may greatly affect their electrochemical properties. However, to the best of our knowledge, there is no report on the electrochemical properties of Co/CMK-3 composite as negative electrode material for Ni/Co battery.

Based on above considerations, we think that CMK-3, as a potential inactive matrix material, is hopeful to improve the electrochemical properties of Ni/Co battery. In this paper, Co/CMK-3 composites are synthesized via a facile hydrothermal reduction route, in which CMK-3 is used as a matrix material. The structural and electrochemical characteristics of Co/CMK-3 composites are investigated in detail. Moreover, the function mechanism is also proposed.

2. Experimental

2.1. Synthesis of CMK-3

The synthesis of CMK-3 was carried out using SBA-15 silica as the hard template and sucrose as the carbon source following the synthesis procedure described by Jun et al. [27]. The preparation of the SBA-15 silica is based on the synthesis procedure first reported by Zhao et al. [28,29].

2.2. Synthesis of Co/CMK-3

Co/CMK-3 composites were synthesized through a hydrothermal route. In a typical synthesis, $CoCl_2 \cdot 6H_2O$ (3 mmol) and CTAB (1 mmol) were dissolved in 70 mL deionized water by ultrasonication for 1 h. Then, different content of CMK-3 (20 mg, 25 mg, and 30 mg) was dispersed in the obtained solution by ultrasonication for 30 min. After hydrazine monohydrate (80% v/v, 10 mL) was added, the solution was stirred and then transferred into a 100 mL Teflon-lined stainless steel autoclave. The autoclave was maintained at 180 °C for 5 h (heating ramp: 2 °C min^{-1}) and then was cooled to room temperature. The final product was collected and washed with distilled water and absolute ethanol for several times, then the product was dried in vacuum at 50 °C overnight. In order to contrast, the pure Co sample was synthesized under same conditions without CMK-3.

2.3. Characterization

The crystal structure and surface morphology of the as-prepared samples were investigated by X-ray diffraction (XRD, Rigaku D/Max-2500, Cu Kα radiation), scanning electron microscopy (SEM, JEOL JSM-6700F), transmission electron microscope (TEM, Philips Tecnai G2 F20 equipped with an energy dispersive X-ray spectrometer (EDX)). The BET surface area was measured by NOVA 2000. The chemical composition was observed by elemental analysis (EA, Perkin–Elmer 2400 Series II CHNS/O).

The electrode was fabricated by a smear method. It was constructed by mixing the prepared material with carbonyl nickel powders and PTFE in a weight ratio of 25:75:5 (0.1 g prepared material) to form a paste and coated on a piece of Ni-foam. Then, the electrode plate was pressed under 5 MPa of pressure for 30 s.

Electrochemical measurements were conducted in a three compartment cell using a Land battery test instrument (CT 2001A). $NiOOH/Ni(OH)_2$ and Hg/HgO were used as the counter electrode and the reference electrode, respectively. The electrolyte was a 6 M KOH aqueous solution. The electrodes were charged at 200 mA g^{-1} for 3 h, discharged to −0.5 V (vs. Hg/HgO) at different current densities after resting for 5 min at room temperature.

The cyclic voltammetry (CV) was conducted by using electrochemical workstation (Zahner IM6e). The potential scan rate was 0.2 mV s^{-1} and the scan scope was −1.2 V to −0.4 V.

3. Results and discussion

3.1. Characterization of structure and morphology

Fig. 1 shows the XRD patterns of the CMK-3, pure Co and Co/CMK-3 (25 mg CMK-3) composite. Small angle X-ray diffraction (SAXRD) measurement is performed on the CMK-3 carbon template (as shown in the inset of Fig. 1), indicating the nature of mesoporous structure of CMK-3. As shown in Fig. 1, the Co/CMK-3 (25 mg CMK-3) composite shows that all diffraction peaks can be readily indexed to the phases of the pure Co and the CMK-3. In addition, the width of Co peaks increases and intensity decreases. It may attribute to the decrease in Co crystallite size and increase in microstrain due to the addition of CMK-3. The diffraction peaks of CMK-3 in Co/CMK-3 (25 mg CMK-3) composite are relatively weak, because the content of CMK-3 is low.

Nitrogen isothermal adsorption–desorption measurements are performed to determine the pore structure and the Brunauer–Emmett–Teller (BET) surface areas of the CMK-3 template, metallic Co and the Co/CMK-3 composites. The BET surface areas are 1098 m^2 g^{-1} for CMK-3 template, 8.90 m^2 g^{-1} for metallic Co, 40.69 m^2 g^{-1} for Co/CMK-3 (20 mg CMK-3) composite, 56.77 m^2 g^{-1} for Co/CMK-3 (25 mg CMK-3) composite and 63.78 m^2 g^{-1} for Co/CMK-3 (30 mg CMK-3) composite, respectively. Obviously, the specific surface area of Co/CMK3 (except CMK-3) is clearly improved by increasing the additive amount of CMK-3, confirming that the CMK-3 successfully loads in the metallic Co. We conclude that CMK-3 worked as a current collector, meanwhile, CMK-3 with high surface area and its hierarchical structure contribute to the increase in surface area.

The morphology and microstructure of the CMK-3, pure Co and Co/CMK-3 (25 mg CMK-3) composite are analysed by field emission scanning electron microscope (FESEM). As shown in Fig. 2a, CMK-3 depicts a worm-like morphology and porous structure. The size of Co particles (Fig. 2b) is about 1.5 μm, and the Co spheres are composed of a number of nanoplates. After loading the CMK-3, Co/CMK-3 (25 mg CMK-3) composite (Fig. 2c) maintains the same shape and morphology as that of the Co particles, except for that the surface is smoother than Co particles and some CMK-3 loads on the surface of Co particles. It indicates that the CMK-3 influences the growth and
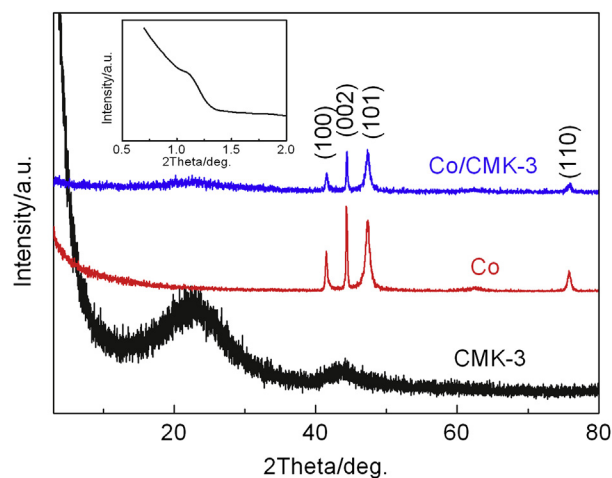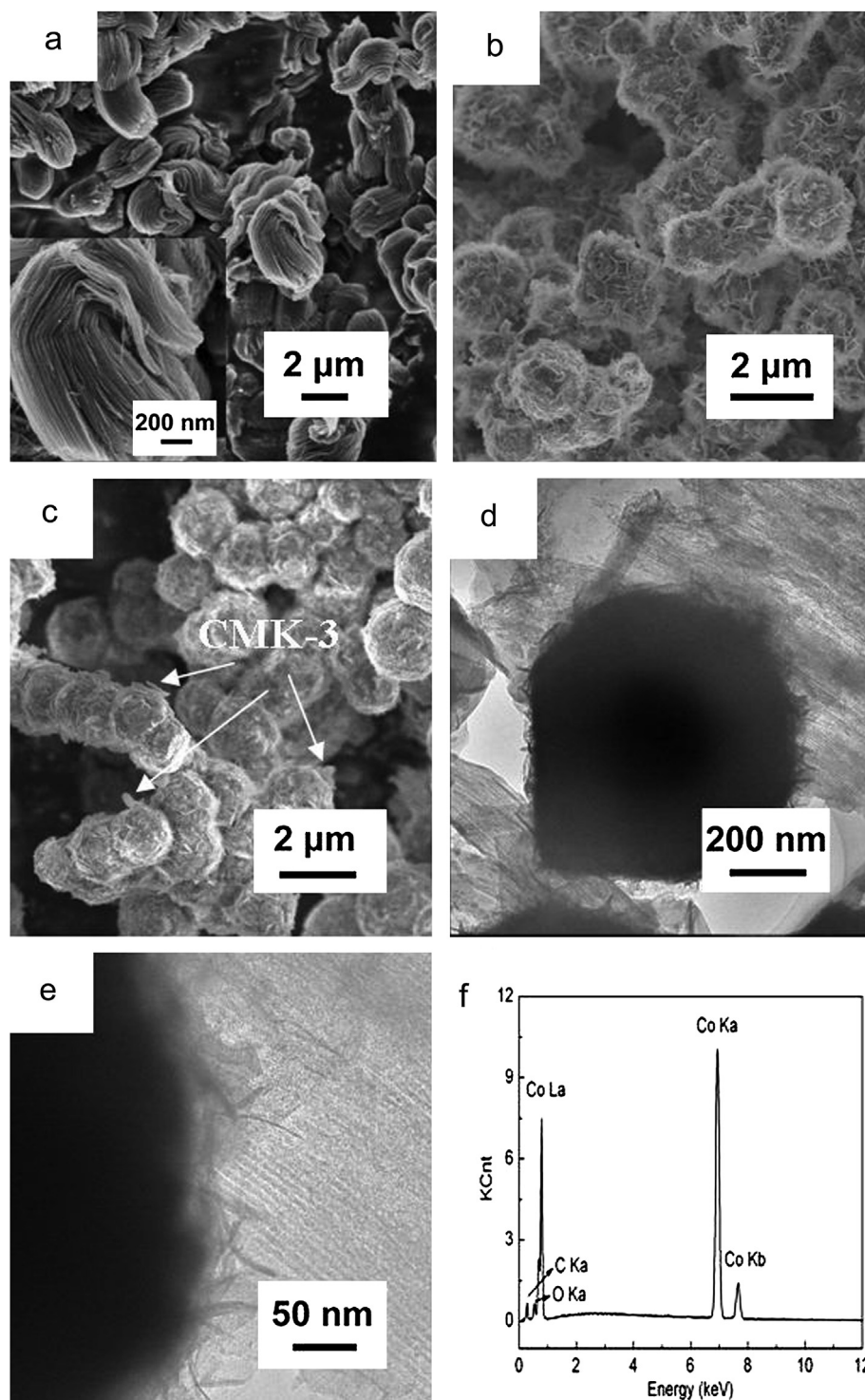

Fig. 1. XRD patterns of the CMK-3, pure Co and Co/CMK-3 (25 mg CMK-3) composite. The inset is the SAXRD pattern of the original CMK-3.

Fig. 2. SEM images of the CMK-3 (a), pure Co (b) and Co/CMK-3 (25 mg CMK-3) composite (c). TEM image of Co/CMK-3 (25 mg CMK-3) composite (d and e). EDX patterns of Co/CMK-3 (25 mg CMK-3) composite (f).

agglomerate of the Co crystallites. Fig. 2c shows that flakes of CMK-3 are deposited on Co particles, which must be supported by Fig. 2d and e. TEM images of Fig. 2d and e also further confirm that Co spheres are composed of a number of nanoplates. The weight percentage of CMK-3 loading in Co particles is determined to be 4.82 wt % by EA. To further confirm the composition of the product, EDX analysis of Co/CMK-3 (25 mg CMK-3) composite is performed. As shown in Fig. 2f, the carbon content of Co/CMK-3 (25 mg CMK-3)

composite is 4.65 wt%, which is consistent with the result obtained by EA. It also demonstrates that the main composition of the Co/CMK-3 (25 mg CMK-3) composite is metallic Co.

3.2. Electrochemical performances of Co/CMK-3 composites

Fig. 3 shows the cycle life of the CMK-3, pure Co and Co/CMK-3 composites (different additive amount of CMK-3) at a discharge
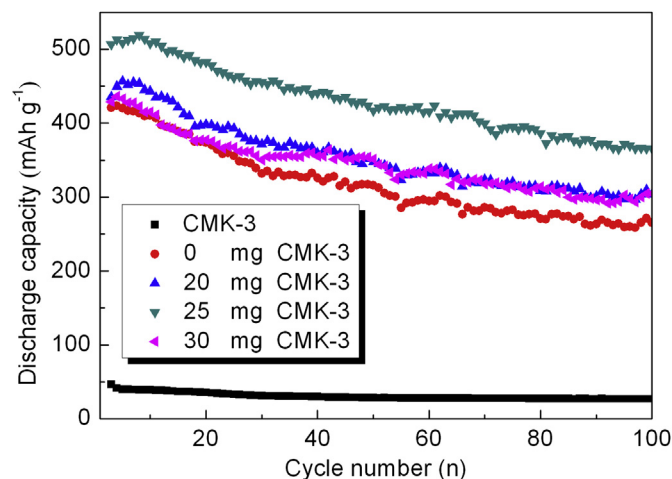
Fig. 3. Cycle life of the CMK-3, pure Co and Co/CMK-3 composites (different additive amount of CMK-3) electrodes.
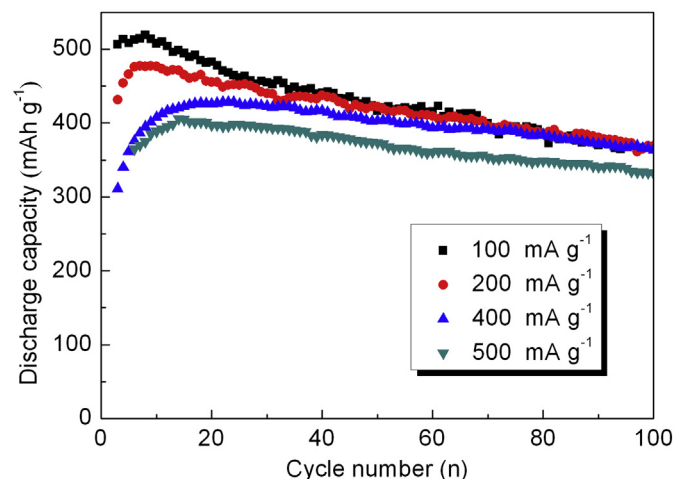

Fig. 4. Cycle life of the Co/CMK-3 composite (25 mg CMK-3) electrode at different discharge current densities.

current density of 100 mA g^{-1}. As shown in Fig. 3, the discharge capacity of the CMK-3 electrode is near 0. Thus, as-synthesized CMK-3 can be regarded as an inactive matrix. For the Co and Co/CMK-3 electrodes, they have an electrochemical activation process. And it is also found that the discharge capacity of Co/CMK-3 electrode increases with increasing the additive amount of CMK-3. When the additive amount of CMK-3 is 25 mg, the discharge capacity reaches the maximum then decreases. We can conclude that adding too many CMK-3 is not helpful to enhance the electrochemical properties of alkaline rechargeable batteries, which may lead to decrease of the active material density in negative electrode. The maximum capacity of the Co electrode is only 423.5 mAh g^{-1} and the capacity decreases to 265.6 mAh g^{-1} after 100 cycles, with the capacity retention rate (C_{100}/C_{max}) of 62.7%. For Co/CMK-3 electrode (25 mg CMK-3), it shows the maximum discharge capacity of 519.3 mAh g^{-1}. After 100 cycles, the discharge capacity still remains at 365.8 mAh g^{-1}, with the capacity retention rate (C_{100}/C_{max}) of 70.4%. Interestingly, discharge capacity is higher than other Co–carbon (Co–CNTS) materials [16,17]. We conclude that CMK-3, as a current collector, can not only improve the dispersion of materials, but also increase the contact area between alkaline solution and active material. Because the charge capacity and discharge capacity of Co-based materials depend on the contact content between alkaline solution and Co-based materials [23]. These results led us believe that the addition of CMK-3 can significantly improve the electrochemical performances of the Co and lead to a remarkable enhancement of the discharge capacity and cycle stability.

The kinetic characteristic of the Co/CMK-3 electrode is investigated by measuring the rate capability at different discharging currents. Fig. 4 shows the cycle life of the Co/CMK-3 (25 mg CMK-3) electrode at the current densities 100, 200, 400 and 500 mAh g^{-1}. It is obvious that the reversible discharge capacity slightly decreases with a corresponding increase of current density. Interestingly, Co/CMK-3 (25 mg CMK-3) electrode shows excellent cycle stability at a discharge current density of 500 mA g^{-1}. These results demonstrate that the Co/CMK-3 (25 mg CMK-3) electrode has an excellent rate capability, further implying that it is a promising anode material for alkaline secondary batteries.

Fig. 5 shows the charge–discharge curves of the Co/CMK-3 (25 mg CMK-3) electrode at the initial several cycles. It is obvious that the initial discharge capacity is 394.7 mAh g^{-1}, then it reaches maximum discharge capacity of 519.3 mAh g^{-1} (the 8th cycle). As

seen from Fig. 5, there is one potential plateau in the discharge curves and two potential plateaus in the charge curves for each cycle. And all the discharge potential plateaus appear at around −0.78 V (vs. Hg/HgO). The first charge potential plateaus appear at around −0.88 V, and the second one only corresponds to electrolysis reaction of water.

Fig. 6 illustrates the CV curves of the Co/CMK-3 (25 mg CMK-3) electrode in the first five cycles. It can be found that a pair of remarkable cathodic and anodic current peaks can be found for each CV curve, and reduction–oxidation peaks appear at −1.038 V and −0.695 V in the fifth CV cycle. Besides, the curve shape and peak voltage of the Co/CMK-3 (25 mg CMK-3) electrode are very similar to the Co-based electrode material [30], suggesting that the same reversible reaction occurs on the electrode. As shown in Fig. 6, the integral area of the redox peaks gradually increase, implying that discharge capacity gradually increases in the first five cycles. The result is consistent with the measurements of cycle performances.

To further investigate the charge–discharge reaction mechanism of the Co/CMK-3, XRD patterns of the Co/CMK-3 electrode
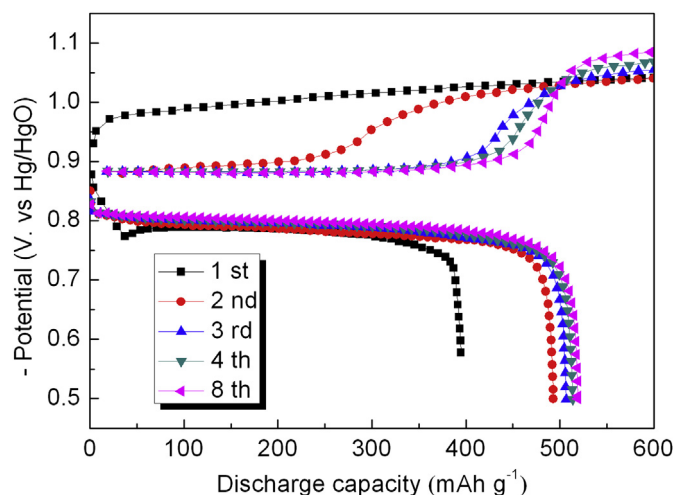

Fig. 5. Charge–discharge curves of the Co/CMK-3 composite (25 mg CMK-3) electrode in the initial cycles.
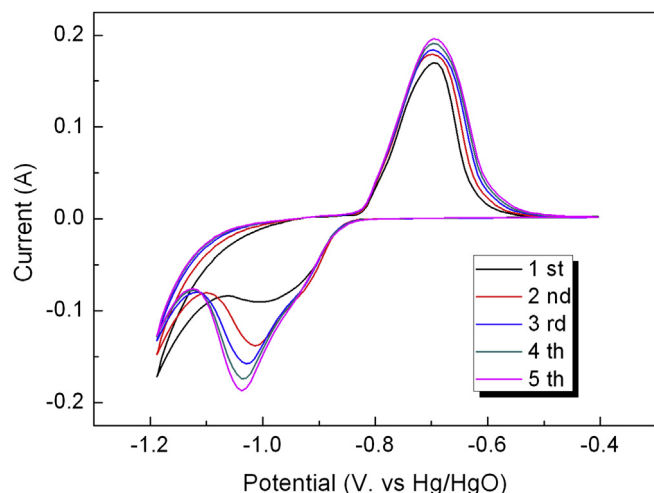
Fig. 6. CV curves of the Co/CMK-3 composite (25 mg CMK-3) electrode in the first five cycles.

Fig. 8. Impedance Nyquist plots of the Co/CMK-3 composite (25 mg CMK-3) and Co electrodes at open circuit potential.

(25 mg CMK-3) at different charge—discharge states are illustrated in Fig. 7. In order to avoid the influence of the Ni diffraction peaks, XRD measurements of the electrodes are prepared with acetylene black as conductive agent. As shown in Fig. 7, only little $Co(OH)_2$ coexists with Co at the fully charged state in the first cycle. Meanwhile, a little amount of Co still coexists with $Co(OH)_2$ at the fully discharged state in the first cycle. Additionally, at the fully charged state in the second cycle, the $Co(OH)_2$ phase is also detected as the coexisting phase with metallic Co. It indicates a partially irreversible conversion between the metallic Co and $Co(OH)_2$ in the Faradaic reaction, leading to the low utilization rate of the metallic Co hierarchitectures. In addition, the diffraction intensity of $Co(OH)_2$ gradually increases at the fully discharged state, implying that the redox irreversibility of metallic Co increases gradually with cycling. It is consistent with the low capacity retention rate. Based on the analyses above, we can attribute the discharge capacity of Co/CMK-3 sample to the redox reaction between Co and $Co(OH)_2$ [16,17,23,31,32]. That is to say, $Co(OH)_2$ is reduced to metallic Co during the charge process, and metallic Co is oxidized to $Co(OH)_2$ during the discharge process. It can be expressed as follows:
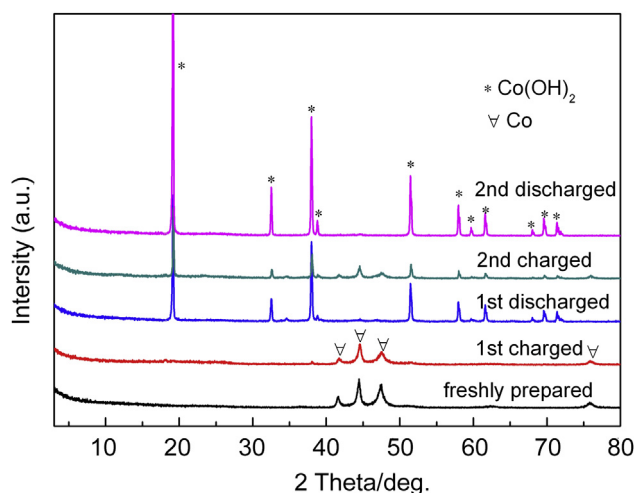
$$Co + 2OH^- \underset{charge}{\overset{discharge}{\rightleftharpoons}} Co(OH)_2 + 2e \qquad (1)$$

In order to further understand the electrochemical performance of Co/CMK-3 electrode, electrochemical impedance spectrum (EIS) is carried out by applying an AC voltage with 5 mV amplitude in a frequency range from 0.1 Hz to 100 kHz. The spectrum of the two electrodes consists of one semicircle and a sloped straight line. The semicircle in high frequency region is ascribed to the charge-transfer or electrochemical reaction resistance (R1), and the low frequency straight line is attributed to the Warburg impedance (W1). As shown in Fig. 8, the diameter of the semicircle in high-frequency becomes small with the introduction of CMK-3, which suggests that the charge-transfer resistance of the Co/CMK-3 electrode decreases. It indicates that the CMK-3 provides excellent electrochemical catalytic activity and promotes the charge-transfer reaction between Co and $Co(OH)_2$.

4. Conclusions

In summary, we have demonstrated the synthesis and application of Co/CMK-3 composites. Electrochemical investigations indicate that the as-synthesized Co/CMK-3 electrodes exhibit favourable properties as negative materials for alkaline rechargeable Ni/Co batteries. The discharge capacity firstly increases with increasing the additive amount of CMK-3, then decreases. The maximum discharge capacity of the Co/CMK-3 (25 mg CMK-3) electrode can reach 519.3 mAh g^{-1}. The high discharge capacity, excellent cycle stability and rate capability clearly demonstrate that mesoporous Co/CMK-3 composites are suitable negative materials for high power applications. In addition, the faradic reaction of Co/CMK-3 electrode between Co and $Co(OH)_2$ is dominated which can be attributed to the dissolution—precipitation mechanism of Co in alkaline solution.

Fig. 7. XRD patterns of the Co/CMK-3 composite (25 mg CMK-3) electrode at charged or discharged states after different cycles.

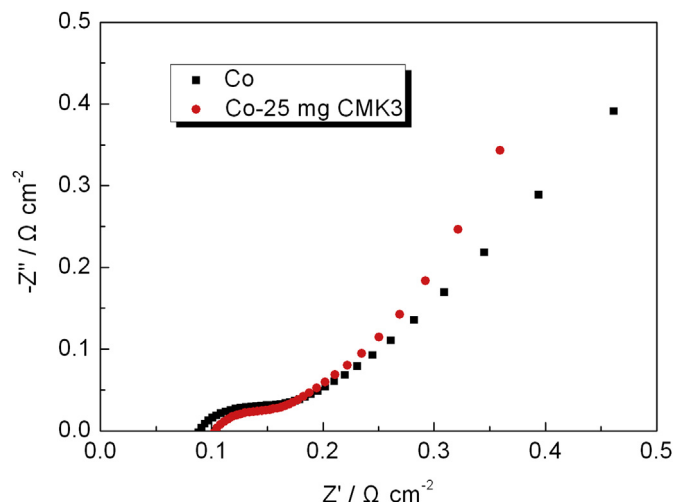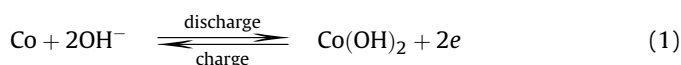## References

[1] X.P. Gao, S.M. Yao, T.Y. Yan, Z. Zhou, Energy Environ. Sci. 2 (2009) 502—505.

[2] Y.D. Wang, X.P. Ai, H.X. Yang, Chem. Mater. 16 (2004) 5194—5197.
[3] Y. Liu, Y.P. Wang, L.L. Xiao, D.W. Song, L.F. Jiao, H.T. Yuan, Electrochem. Commun. 9 (2007) 925—929.
[4] X.Y. Zhao, L.Q. Ma, X.D. Shen, J. Mater. Chem. 22 (2012) 277—285.
[5] V.F. Puntes, K.M. Krishnan, A.P. Alivisatos, Science 291 (2001) 2115—2117.
[6] S.R. Chung, K.W. Wang, M.H. Teng, T.P. Perng, Int. J. Hydrogen Energy 34 (2009) 1383—1388.
[7] D.S. Lu, W.S. Li, C.L. Tan, R.H. Zeng, Electrochim. Acta 55 (2009) 171—177.
[8] C.C. Li, H.C. Zeng, J. Mater. Chem. 20 (2010) 9187—9192.
[9] Y. Wang, J.M. Lee, X. Wang, Int. J. Hydrogen Energy 35 (2010) 1669—1673.
[10] Y. Liu, Y.J. Wang, L.L. Xiao, D.W. Song, Y.P. Wang, L.F. Jiao, H.T. Yuan, Electrochim. Acta 53 (2008) 2265—2271.
[11] Y.L. Cao, W.C. Zhou, X.Y. Li, X.P. Ai, X.P. Gao, H.X. Yang, Electrochim. Acta 51 (2006) 4285—4290.
[12] D.W. Song, Q.H. Wang, Y.P. Wang, Y.J. Wang, Y. Han, L. Li, G. Liu, L.F. Jiao, H.T. Yuan, J. Power Sources 195 (2010) 7462—7465.
[13] Q.H. Wang, L.F. Jiao, Y. Han, H.M. Du, W.X. Peng, Q.N. Huan, D.W. Song, Y.C. Si, Y.J. Wang, H.T. Yuan, J. Phys. Chem. C 115 (2011) 8300—8304.
[14] Z.W. Lu, S.M. Yao, G.R. Li, T.Y. Yan, X.P. Gao, Electrochim. Acta 53 (2008) 2369—2375.
[15] D.W. Song, Y.N. Xu, C.H. An, Q.H. Wang, Y.P. Wang, L. Li, Y.J. Wang, L.F. Jiao, H.T. Yuan, Phys. Chem. Chem. Phys. 14 (2012) 71—75.
[16] Y. Han, Y.J. Wang, Y.P. Wang, L.F. Jiao, H.T. Yuan, S.X. Liu, Electrochim. Acta 56 (2011) 3258—3263.
[17] H.M. Du, L.F. Jiao, Q.H. Wang, W.X. Peng, D.W. Song, Y.J. Wang, H.T. Yuan, J. Power Sources 196 (2011) 5751—5755.
[18] B. Sun, Z.X. Chen, H.S. Kim, H.J. Ahn, G.X. Wang, J. Power Sources 196 (2011) 3346—3349.
[19] K. Chang, W.X. Chen, J. Mater. Chem. 21 (2011) 17175—17184.
[20] X.L. Ji, S. Evers, K.T. Lee, L.F. Nazar, Chem. Commun. 46 (2010) 1658—1660.
[21] H.S. Zhou, S.M. Zhu, M. Hibino, I. Honma, M. Ichihara, Adv. Mater. 15 (2003) 2107—2111.
[22] G.X. Wang, H. Liu, J. Liu, S.Z. Qiao, G.Q. Max Lu, P. Munroe, H. Ahn, Adv. Mater. 22 (2010) 4944—4948.
[23] D.W. Song, Y.P. Wang, Q.H. Wang, Y.J. Wang, L.F. Jiao, H.T. Yuan, J. Power Sources 195 (2010) 7115—7119.
[24] Q.H. Wang, L.F. Jiao, H.M. Du, W.X. Peng, D.W. Song, Y.J. Wang, H.T. Yuan, Electrochim. Acta 56 (2011) 1106—1110.
[25] Q.H. Wang, L.F. Jiao, H.M. Du, Q.N. Huan, W.X. Peng, D.W. Song, Y.J. Wang, H.T. Yuan, J. Mater. Chem. 21 (2011) 14159—14162.
[26] C.M. Doherty, R.A. Carusoab, C.J. Drummond, Energy Environ. Sci. 3 (2010) 813—823.
[27] S. Jun, S.H. Joo, R. Ryoo, M. Kruk, M. Jaroniec, Z. Liu, T. Ohsuna, O. Terasaki, J. Am. Chem. Soc. 122 (2000) 10712—10713.
[28] D. Zhao, J. Feng, Q. Huo, N. Melosh, G.H. Fredrickson, B.F. Chmelka, G.D. Stucky, Science 279 (1998) 548—552.
[29] D. Zhao, Q. Huo, J. Feng, B.F. Chmelka, G.D. Stucky, J. Am. Chem. Soc. 120 (1998) 6024—6036.
[30] S.M. Yao, K. Xi, G.R. Li, X.P. Gao, J. Power Sources 184 (2008) 657—662.
[31] P. Elumalai, H.N. Vasan, N. Munichandraiah, J. Power Sources 93 (2001) 201—208.
[32] B.S. Haran, B.N. Popov, R.E. White, J. Electrochem. Soc. 145 (1998) 3000—3007.